

Regulatory Blueprint for a Chordate Embryo

Kaoru S. Imai *et al.*

Science 312, 1183 (2006);

DOI: 10.1126/science.1123404

This copy is for your personal, non-commercial use only.

If you wish to distribute this article to others, you can order high-quality copies for your colleagues, clients, or customers by [clicking here](#).

Permission to republish or repurpose articles or portions of articles can be obtained by following the guidelines [here](#).

The following resources related to this article are available online at www.sciencemag.org (this information is current as of August 5, 2013):

Updated information and services, including high-resolution figures, can be found in the online version of this article at:

<http://www.sciencemag.org/content/312/5777/1183.full.html>

Supporting Online Material can be found at:

<http://www.sciencemag.org/content/suppl/2006/05/23/312.5777.1183.DC1.html>

A list of selected additional articles on the Science Web sites related to this article can be found at:

<http://www.sciencemag.org/content/312/5777/1183.full.html#related>

This article cites 27 articles, 14 of which can be accessed free:

<http://www.sciencemag.org/content/312/5777/1183.full.html#ref-list-1>

This article has been cited by 94 article(s) on the ISI Web of Science

This article has been cited by 42 articles hosted by HighWire Press; see:

<http://www.sciencemag.org/content/312/5777/1183.full.html#related-urls>

This article appears in the following subject collections:

Development

<http://www.sciencemag.org/cgi/collection/development>

16. K. Lee, E. J. Weinberg, *Phys. Rev. D* **36**, 1088 (1987).
17. S. W. Hawking, I. G. Moss, *Phys. Lett. B* **110**, 35 (1983).
18. S. J. Parke, *Phys. Lett. B* **21**, 313 (1983).
19. J. Khoury, B. A. Ovrut, P. J. Steinhardt, N. Turok, *Phys. Rev. D* **64**, 123522 (2001).
20. G. Felder, A. Frolov, L. Kofman, A. Linde, *Phys. Rev. D* **66**, 023507 (2002).
21. J. Khoury, P. J. Steinhardt, N. Turok, *Phys. Rev. Lett.* **92**, 031302 (2004).
22. P. Creminelli, A. Nicolis, M. Zaldarriaga, *Phys. Rev. D* **71**, 063505 (2005).
23. T. J. Battefeld, S. P. Patil, R. Brandenberger, *Phys. Rev. D* **70**, 066006 (2004).
24. P. McFadden, N. Turok, P. J. Steinhardt, published online 12 December 2005 (<http://arxiv.org/pdf/hep-th/0512123>).
25. L. A. Boyle, P. J. Steinhardt, N. Turok, *Phys. Rev. D* **69**, 127302 (2004).
26. For a recent discussion, see P. Fox, A. Pierce, S. Thomas, published online 3 September 2004 (<http://arxiv.org/pdf/hep-th/0409059>).
27. M. S. Turner, F. Wilczek, *Phys. Rev. Lett.* **40**, 279 (1978).
28. A. D. Linde, *Phys. Lett. B* **259**, 38 (1991).
29. M. Tegmark, A. Aguirre, M. J. Rees, F. Wilczek, *Phys. Rev. D* **73**, 023505 (2006).
30. T. Banks, M. Dine, N. Seiberg, *Phys. Lett. B* **273**, 105 (1991).

14 February 2006; accepted 28 March 2006
 Published online 4 May 2006;
 10.1126/science.1126231
 Include this information when citing this paper.

Regulatory Blueprint for a Chordate Embryo

Kaoru S. Imai,¹ Michael Levine,² Nori Satoh,¹ Yutaka Satou^{1*}

Ciona is an emerging model system for elucidating gene networks in development. Comprehensive *in situ* hybridization assays have identified 76 regulatory genes with localized expression patterns in the early embryo, at the time when naïve blastomeres are determined to follow specific cell fates. Systematic gene disruption assays provided more than 3000 combinations of gene expression profiles in mutant backgrounds. Deduced gene circuit diagrams describing the formation of larval tissues were computationally visualized. These diagrams constitute a blueprint for the *Ciona* embryo and provide a foundation for understanding the evolutionary origins of the chordate body plan.

During the past three decades, there has been remarkable progress in identifying the regulatory genes and signaling pathways responsible for the development of a variety of tissues and organs in worms, fruit flies, sea urchins, zebrafish, frogs, chicks, and mice. However, there are just a few cases where this information has been integrated to produce gene regulation networks embodying the functional interconnections among the genes responsible for a given developmental process. The best success has been obtained for the specification of endomesoderm in the pregastrular sea urchin embryo (1) and the dorsal-ventral patterning of the early *Drosophila* embryo (2). Significant progress has also been made on the specification of the “Spemann organizer” in the *Xenopus* embryo (3).

The ascidian *Ciona intestinalis* provides an ideal experimental system to elucidate gene regulatory networks. The ascidian tadpole shares a common body plan with vertebrates (4), including a notochord centered in the tail that is flanked dorsally by the nerve cord, laterally by muscle, and ventrally by endoderm. The mature ascidian larva is composed of ~2600 cells, and the genome contains only 16,000 genes (5). This genetic and cellular simplicity offers the promise of superimposing gene networks onto the behav-

ior of individual cells during specification and differentiation in early embryos. Such networks would provide a detailed understanding of complex morphogenetic processes and would establish a foundation for determining the evolutionary origins of chordate features in lower Deuterostomes (e.g., starfish and acorn worms) and their subsequent elaboration in vertebrates.

Here we present the systematic analysis of the 76 zygotic regulatory genes controlling *Ciona* embryogenesis during the time when the basic chordate tissues are specified and begin to differentiate. Particular efforts focus on the transcription factors and signaling components dedicated to the major tissues of the early tadpole. *Macho-1*, *Tbx6b*, and *ZicL* are expressed in the tail muscles (6–9); *β-catenin* and *Lhx3* in the endoderm (10, 11); *Fgf9/16/20*, *FoxA-a*, *FoxD*, *ZicL*, and *Brachury* in the notochord (7, 12–14); and *Fgf9/16/20*, *Nodal*, *Otx*, and *GATA-a* in the CNS (15, 16). Gene disruption and *in situ* hybridization assays were used to create circuit diagrams showing the functional interconnections among the signaling pathways and regulatory factors governing the dynamic cellular interactions underlying the formation of the nerve cord, notochord, heart, and other key chordate tissues. These circuit diagrams constitute a blueprint for *Ciona* embryogenesis.

Regulatory codes for defined lineages.

Previous comprehensive *in situ* hybridization assays showed that the *Ciona* genome contains 65 genes encoding sequence-specific transcription factors (TFs) and 26 genes encoding components of cell signal transduction molecules (STs)

that are zygotically expressed between the 16-cell and early gastrula stages of embryogenesis (17, 18). Because of difficulties measuring zygotic transcription of genes expressed both maternally and zygotically, we excluded those genes exhibiting abundant maternal transcripts, thereby restricting the total to 53 TF genes and 23 ST genes (table S1). We do not regard the exclusion of maternal genes as a major limitation, because they are used to establish a regulatory prepattern in 16-cell embryos. The link between this prepattern and the establishment of definitive larval tissues is the major focus of the present study.

From the 16-cell to early gastrula (around 110-cell) stage, most of the blastomeres can be assigned a unique identity on the basis of the expression of specific combinations of TF genes (regulatory code; summarized in fig. S1). There is a close correspondence between establishing different regulatory codes and forming diverse cell lineages (Fig. 1). For example, the blastomeres that form the primitive gut (endoderm; A6.1, B6.1, and A6.3 at the 32-cell stage; and A7.1, A7.2, A7.5, B7.1, and B7.2 in 64-cell embryos) have slightly different regulatory codes during early cleaving embryos (fig. S2, A and B) but acquire identical codes at the early gastrula stage. The b5.3 and b5.4 blastomeres contain similar regulatory codes at the 16-cell stage. At the gastrula stage, descendants that give rise to nerve cord cells (b8.17 and b8.19) acquire a regulatory code that is distinct from their sister cells that give rise to epidermal cells (b8.18 and b8.20). The latter cells have a code that is similar to those of other epidermal cells, which indicates an inductive event at or before this stage. All lineages except the B7.5 blastomeres, which form the heart (trunk ventral cells) and anterior tail muscles, achieve clonal restriction before gastrulation. Thus, the hierarchical clustering of cell identities with similar regulatory codes accurately reflects cell lineages and the clonal restriction of cell fate and illuminates at what point key molecular interactions occur to establish a unique identity for each cell.

In order to define distinct neuronal cell identities, it was necessary to extend the analysis of regulatory codes beyond the early gastrula stage because of the complexity of neural cell types. Systematic *in situ* hybridization assays suggested that there are at least 13 distinct neuronal cell types composing the future central and peripheral nervous system at the late gastrula stage (Fig. 2, A and B;

*Department of Zoology, Graduate School of Science, Kyoto University, Sakyo-ku, Kyoto, 606-8502, Japan. ²Department of Molecular and Cellular Biology, Division of Genetics and Development, University of California, Berkeley, CA 94720, USA.

*To whom correspondence should be addressed. E-mail: yutaka@ascidian.zool.kyoto-u.ac.jp

fig. S3A). There are also at least six different TF-ST combinations in the epidermis of tailbud stage embryos (Fig. 2C; fig. S3B). The TF-ST codes identified for the neuronal and epidermal cell types in the *Ciona* tadpole could be useful for determining whether comparable cells exist in the diffuse nervous systems of lower Deuterostomes, such as starfish (echinoderms) and acorn worms (hemichordates).

Elucidation of provisional gene networks.

There are five distinct regulatory codes seen for the eight different blastomeres (paired blastomeres are

identical across the left-right axis) in 16-cell embryos (Fig. 1, A and B): anterior animal blastomeres (a-line blastomeres), posterior animal blastomeres (b-line blastomeres), anterior vegetal blastomeres (A-line blastomeres; not identical to each other, but very similar), the posterior vegetal blastomere (B5.1 blastomeres), and the posteriormost blastomere (B5.2). *FoxA-a*, *FoxD*, *Tbx6a*, *Tbx6b/c/d* (fig. S1), and *Fgf9/16/20* (13) display restricted patterns of zygotic expression in 16-cell embryos. These restricted patterns constitute a prepattern that is used to produce

the major larval tissues. For example, *FoxD* makes presumptive notochord cells competent for response to *Fgf9/16/20* by activating *ZicL* expression (see also supporting online text). The link between the 16-cell prepattern and the specification of basic chordate tissues is described below.

Perturbation of TF and ST gene function was achieved by microinjection of morpholino oligonucleotides (MOs; supporting online text) (19). MOs were designed for 70 of the 76 genes (table S2), but 30 of them failed to produce clear mutant phenotypes when microinjected into fertilized eggs (Table 1). Four of the MOs severely slowed cleavage; another nine produced additional nonspecific defects. The remaining 27 MOs produced unambiguous and specific mutant phenotypes (Table 1). The identification of specific mutant phenotypes for 27 of 70 MOs (~40%) is consistent with previously reported “hit-rates” using single MOs for a given gene (20).

Quantitative reverse transcription–polymerase chain reaction (qRT-PCR) assays were used to examine the expression profiles of 73 of the 76 TF and ST genes in 25 of the 27 mutants at the early gastrula stage (21) (table S3; fig. S4). In situ hybridization assays were used to determine the detailed expression profiles of subsets of the TF and ST genes in select mutant backgrounds (table S4; figs. S5 and S6). In addition, 39 TF and 12 ST genes were similarly examined in the 27 mutants at the late gastrula stage (tables S4 and S5; figs. S5, S6, and S7). Finally, 16 mutants were examined at tailbud stages using 17 different TF and ST in situ hybridization probes (table S4; figs. S5 and S6). Overall, the resulting analysis provided more than 3000 combinations of gene expression profiles and mutant backgrounds. This information, along with earlier results, was used to create a provisional circuit diagram showing the interconnections among 79 TF and 25 ST genes controlling cell-fate specification and the initial phases of tissue differentiation (Fig. 3A).

The entire analysis of TF and ST expression profiles in MO mutant embryos is available on a World Wide Web interface [(22) or Database S1]. The circuit diagrams are illustrated for individual blastomeres in successively older embryos extending to the early gastrula stage. At later stages, the diagrams encompass groups of cells forming discrete tissues.

Circuit diagram for the notochord. The prepattern seen in 16-cell embryos establishes the presumptive notochord through the activation of *Brachyury* expression. *Brachyury* encodes a T-box transcription factor that regulates a variety of target genes controlling the cell shape changes and intercalary movements accompanying notochord differentiation (23).

The anterior 32 notochord cells arise from the A7.3 and A7.7 blastomeres at the 64-cell stage. A-line activation depends on *ZicL* and *Fgf9/16/20* (7, 13) (Fig. 3B). *Fgf9/16/20* signaling may be mediated by phosphorylation of the ETS-containing transcription factor, ets/pointed2. *ZicL*

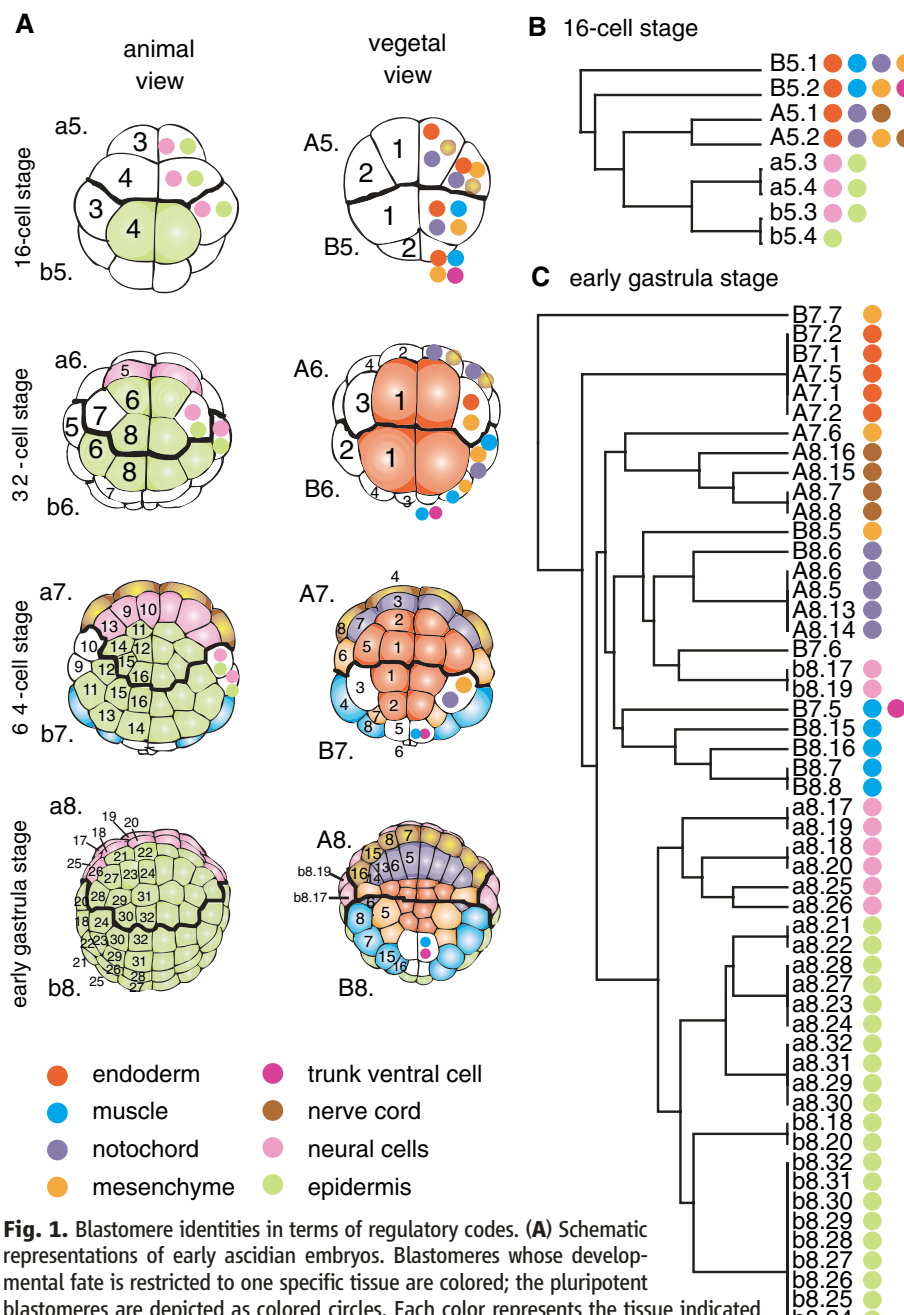


Fig. 1. Blastomere identities in terms of regulatory codes. **(A)** Schematic representations of early ascidian embryos. Blastomeres whose developmental fate is restricted to one specific tissue are colored; the pluripotent blastomeres are depicted as colored circles. Each color represents the tissue indicated at the bottom. The names of individual cells indicated in each illustration should be prefixed with IDs shown at the left. The anterior and posterior boundaries are shown as thick lines. **(B and C)** Hierarchical clusterings of blastomeres based on regulatory codes at the 16-cell (**B**) and early gastrula (**C**) stages. The developmental potentials of each cell are shown with the same color codes as in **(A)**.

activated in the A-line progenitors by *FoxA-a* and *FoxD* (fig. S5, A and B), two of the early determinants of the 16-cell prepattern. It is conceivable that *FoxA-a* and *ZicL* function through a feed-forward loop, which is a common feature of previously characterized gene regulatory networks, including those controlling endomesoderm formation in sea urchin embryos and dorsal-ventral patterning of the *Drosophila* embryo (1, 2). *FoxA-a* is expressed in the A-line progenitors at the 32-cell stage, A6.2 and A6.4. Expression persists in A7.3 and A7.7, but not in A7.4 and A7.8, which form A-line nerve cord derivatives (fig. S1). This asymmetric activity of *FoxA-a* might exclude *Brachyury* expression in nerve cord cells. The posterior eight notochord cells arise from the B8.6 blastomeres, where *Brachyury* is also activated by a distinct mechanism (see below; supporting online text).

The nodal network. Nodal is a member of the transforming growth factor β (TGF β) superfamily of signaling molecules. It is conserved in Deuterostomes, including sea urchins, ascidians, and vertebrates, but not found in protostomes. In *Xenopus*, *Nodal* and *Nodal-related genes* (XNRs) are expressed predominantly in the dorsal endomesoderm (24). A different function is seen in sea urchins. *Nodal* is expressed in the oral ectoderm, but not endomesoderm, and it patterns the oral-aboral axis (25). The detailed analysis of *Nodal* function in *Ciona* raises the possibility that ascidians have hybrid properties of lower Deuterostomes and vertebrates (Fig. 4).

Nodal is first expressed in the b6.5 blastomere, which gives rise to the b7.9 and b7.10 daughters in 64-cell embryos (Fig. 4A). These cells form dorsal epidermal tissues and the dorsal-most ependymal cells of the nerve cord—the roof cells. The localized expression of *Nodal* depends on at least three regulatory influences. First, *Fgf9/16/20* signals, emanating from a wide range of the A-line and B-line vegetal cells, induce *Nodal* expression in the b6.5 lineage. Second, restricted expression depends on direct or indirect repression by *SoxC* and *FoxA-a* (Fig. 4B). Finally, *Nodal* is negatively autoregulated; there is more than a 10-fold elevation in the levels of expression in mutant embryos injected with the *Nodal* MO. It is highly likely that this auto-regulation is required for supplying the proper amount of *Nodal* ligand to the surrounding cells. Negative feedback loops are a common feature of other gene networks that have been examined (25, 26).

Recent studies suggest that *Nodal* functions as an organizing signal, which patterns the developing nerve cord (16). Considered in cross section, the larval nerve cord contains four ependymal cells surrounding a hollow cord. The ventral-most ependymal cell has the properties of a simple floor plate. It expresses floor plate markers such as *hedgehog-2* (*hh-2*) and *FoxA-a* (*HNF3 β*) (27, 28). MO-mediated knockdown of *SoxC* activity results in ectopic expression of *Nodal* in the a-line neuronal cells and concomitant misexpression of *snail*, *Delta-like*, *Pax6*, *Cdx*, and *Neurogenin* in the floor plate (fig. S5E).

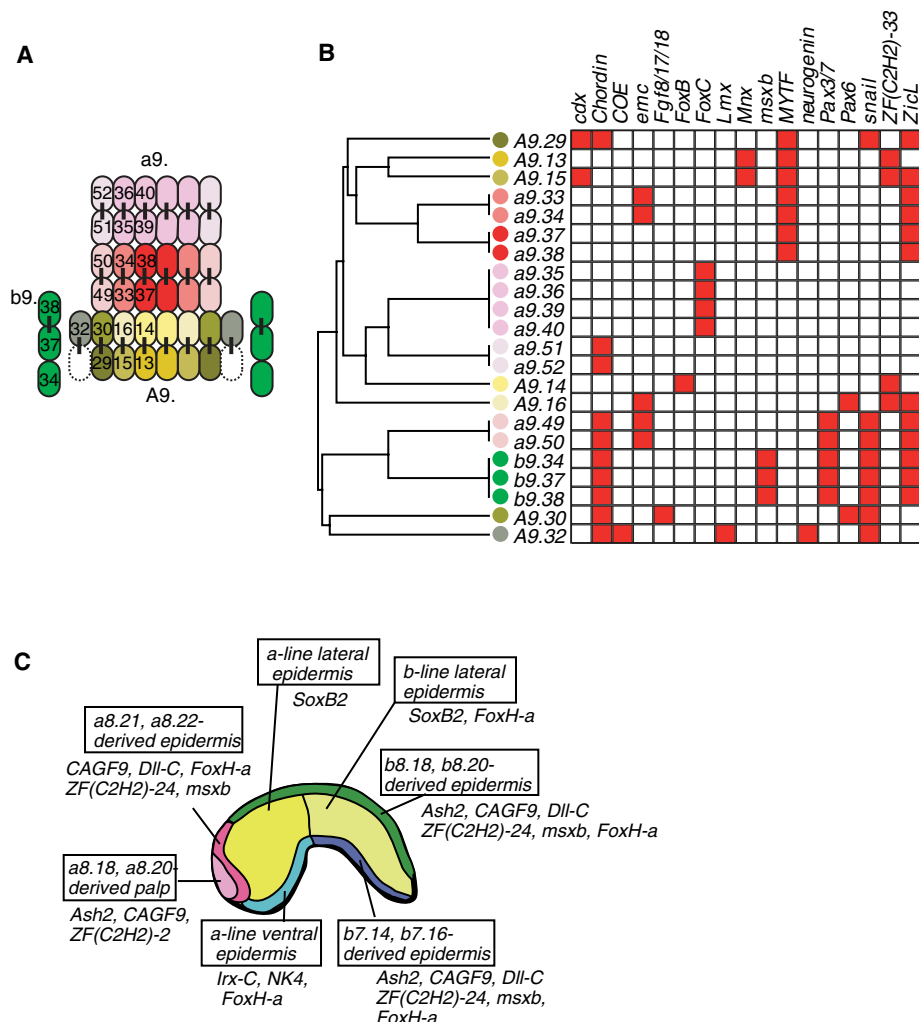


Fig. 2. (A and B) Cell identities in the neural plate at the late gastrula stage, characterized on the basis of the expression profiles of selected TF and ST genes. (A) Cells in the neural plates are shown in colors, with cell identities represented by a color code. The names of individual cells, indicated at the left half of each illustration, should be prefixed with the IDs shown at the outside of the illustration. Vertical bars indicate sister relations between blastomeres. (B) Hierarchical clustering of blastomeres in the neural plate (left) and gene expression profiles (right). The color code of the circles is the same as that used in (A). (C) A schematic representation of the epidermal territories of the tailbud embryo, defined by the expression profiles of 10 TF genes.

Table 1. Summary of knockdown experiments with morpholino oligonucleotides.

Gene	No. of genes
Genes analyzed in detail	
<i>ADMp</i> , <i>AP-2-like2</i> , <i>Brachyury</i> , <i>dickkopf</i> , <i>Dll-B</i> , <i>DMRT1</i> , <i>ets/pointed2</i> , <i>FGF9/16/20</i> , <i>FoxA-a</i> , <i>FoxB</i> , <i>FoxC</i> , <i>FoxD-a/b</i> , <i>lefty/antivin</i> , <i>Mesp</i> , <i>msxb</i> , <i>MyoD</i> , <i>Neurogenin</i> , <i>nodal</i> , <i>NoTlrc</i> , <i>Otx</i> , <i>Snail</i> , <i>SoxC</i> , <i>Tbx2/3</i> , <i>Tbx6b/c/d</i> , <i>Twist-like1a/b</i> , <i>Wnt5</i> , <i>ZicL</i>	27
Genes for which a morpholino oligonucleotide did not give any effects	
<i>BMP2/4</i> , <i>BMP3</i> , <i>E(spl)/hairy-a</i> , <i>ELK</i> , <i>Emc</i> , <i>Eph1</i> , <i>FGF8/17/18</i> , <i>Fli/ERG1</i> , <i>Fli/ERG3</i> , <i>Fos</i> , <i>Fz4</i> , <i>Hedgehog1</i> , <i>HNF4</i> , <i>Irx-B</i> , <i>Lhx3</i> , <i>noggin</i> , <i>Orphan Fox-2</i> , <i>Orphan Wnt-e</i> , <i>RAR</i> , <i>sFRP1/5</i> , <i>SOCS1/2/3/CIS</i> , <i>SoxB1</i> , <i>SoxB2</i> , <i>SoxF</i> , <i>SMYD1</i> , <i>Tbx6a</i> , <i>TGFβ</i> not assigned 1, <i>TTF1</i> , <i>ZF (C2H2)-2</i> , <i>ZF (C2H2)-25</i>	30
Genes for which a morpholino oligonucleotide evoked a nonspecific effect or a phenotype that was not expected from the zygotic gene expression pattern	
<i>DUSP1.2.4.5</i> , <i>E(spl)/hairy-b</i> , <i>E12/E47</i> , <i>EphrinA-c</i> , <i>EphrinA-d</i> , <i>FoxH-b</i> , <i>FoxP</i> , <i>Jun</i> , <i>Mnx</i> , <i>PPAR</i> , <i>ROR</i> , <i>ZF (C2H2)-34</i> , <i>ZF (C3H)</i>	13
Genes for which no cDNA clone could be obtained and that were not examined in this study	
<i>Chordin</i> , <i>Delta-like</i> , <i>GATA-b</i> , <i>MyTF</i> , <i>Otp</i> , <i>Tolloid</i>	6

Nodal activates *Msxb*, *Pax3/7*, *snail*, *Delta-like*, and *Chordin* within the b6.5 lineage that forms the roof nerve cord cells and dorsal epidermis (Fig. 4B). It also induces *Snail*, *Delta-like*, *Neurogenin*, and *E(spl)/Hairy-b* expression in the A7.8 lineage, which forms the lateral ependymal cells of the nerve cord (Fig. 4B). Localized repressors in the lateral cells help restrict gene expression within the floor plate. For example, *Snail* restricts *Mnx* expression to the floor plate and keeps it off in lateral ependymal cells.

The cellular simplicity of the *Ciona* embryo and tadpole permits the elucidation of “four-dimensional” gene networks, whereby cell-autonomous gene cascades can be linked to dynamic signaling interactions between neighboring cells. For example, Nodal emanating from the b6.5 lineage induces *NoTrlc* and *Delta-like* expression in the neighboring trunk lateral cell, A7.6, which gives rise to adult blood cells and muscles (29). It is possible that Delta-like relays Notch signaling in the B7.3 blastomere, which forms the secondary notochord and mesenchyme. Delta is a well-known ligand for the Notch receptor [e.g., (30)], and the primary transcriptional effector of Notch-signaling—Su(H)—replaces the ZicL activator to induce *Brachyury* expression in the B8.6 (secondary) notochord lineage (supporting online text). Thus, the b6.5 lineage has the properties of an organizer. It is essential for the patterning of the nerve cord and the induction of internal mesoderm derivatives, such as the secondary notochord (Fig. 4B).

Transcriptional repression. As in the case of Nodal negative feedback, repression is an important feature of gene networks. For example, the Snail repressor is expressed in the notochord. Earlier, when *Brachyury* is first activated in the A-line and B-line progenitors at the 64-cell stage, the Snail repressor is restricted to the trunk mesenchyme and developing tail muscles (31). *Snail* is activated in the tail muscles and helps exclude *Brachyury* expression in neighboring muscle cells when Delta-like and *Fgf9/16/20* induce notochord formation. However, by the onset of gastrulation, *Snail* is expressed in notochord cells, where it might attenuate *Brachyury* expression. Peak *Brachyury* expression is seen at neurulation, but only low levels persist during elongation of the tail. It is conceivable that this down-regulation is important for normal notochord differentiation, because sustained expression of high levels of *Brachyury* causes defects in notochord intercalation and tail elongation.

Repression is also a prominent feature of other gene regulation networks. For example, the pMar repressor in the sea urchin micromere lineage permits localized expression of a Delta ligand, which induces Notch signaling in neighboring endomesoderm cells (1). Similarly, the Snail repressor in the presumptive mesoderm of early *Drosophila* embryos results in the activation of Notch signaling in neighboring mesectoderm cells in the ventral-most regions of the neurogenic ectoderm (2).

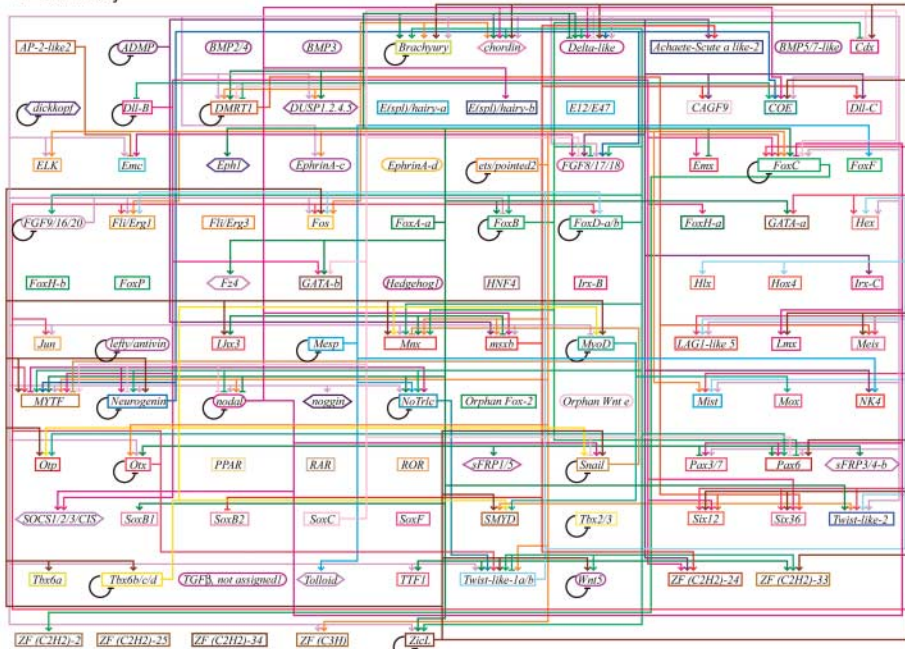
As shown in table S7, 22 of the 27 genes examined in this study negatively regulate themselves, directly or indirectly. Thus, it would ap-

pear that negative autoregulation loops are an essential property of ascidian gene regulatory networks.

Conclusions. The preceding analysis provides provisional circuit diagrams for the specification and initial differentiation of several tissues of the

Ciona tadpole, including the gut, tail muscles, notochord, heart, nerve cord, and brain [supporting online text (fig. S8)]. Definitive gene networks will require integrating this information with lineage-specific enhancers from key patterning genes. For example, the characterization of a

A Summary



B Notochord (A8.5, A8.6) at the early gastrula stage

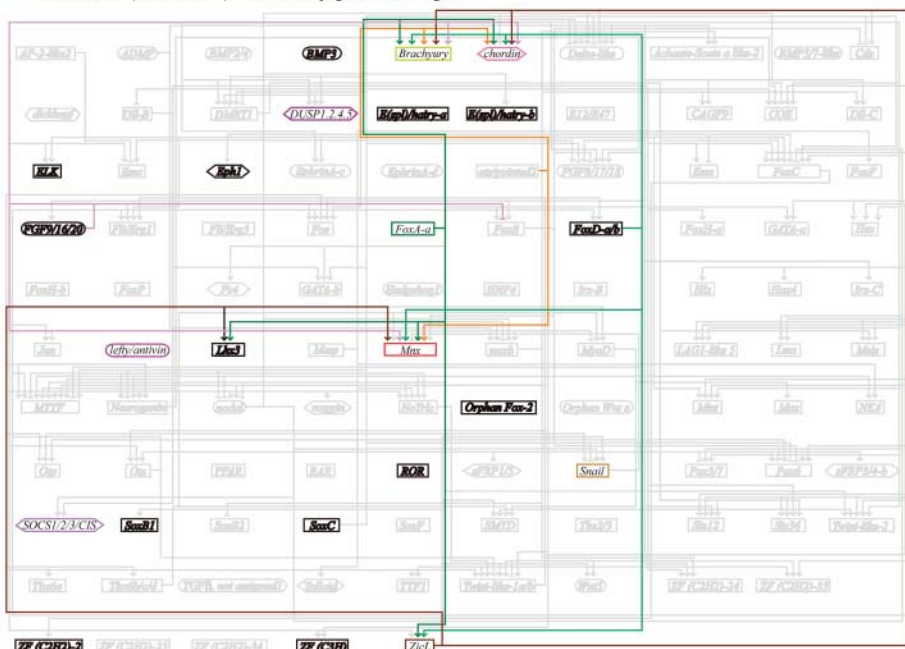


Fig. 3. Gene regulatory networks in the ascidian embryo. **(A)** Summary of all relations. **(B)** Relations in A-line notochord cells at the early gastrula stage. TF genes are indicated by rectangles. Signaling ligand genes and other ST genes are shown by ovals and hexagons. Arrows indicate transcriptionally regulatory interactions. The flat-head arrows indicate repression. Genes expressed in the ancestors of the cell, but not expressed at this stage, are enclosed by a black rectangle. Genes that are not expressed in either the specified cell or its ancestors are shown in light gray.

minimal notochord-specific enhancer from the *Brachury* gene provides evidence that *ZicL*, *Fgf9/16/20*, and Notch jointly establish the prospective notochord, rather than functioning in a sequential pathway (see Fig. 4B).

The current study provides a foundation for determining the evolutionary origins of chordate structures, and their elaboration in vertebrate systems. It also provides insights for evolutionary plasticity and conservation, as ascidians are simple chordates that might retain some of the ancestral properties of the first chordates, as well as emergent properties of vertebrates. The circuit diagrams provide a glimpse of the genetic and cellular interactions that might have operated in the earliest ancestors of the vertebrates. For example, we have argued that Nodal signal emanating from the b6.5 lineage might represent a “transitional organizer,” with hybrid properties seen in sea urchins and vertebrates.

One of the great mysteries in evolutionary biology is the origin of the chordate body plan. The closest nonchordate relatives of ascidians, the hemichordates (e.g., acorn worms) and echinoderms (e.g., starfish), do not display a tadpole-like organization at any point in their life cycles. It should be possible to use the genetic circuits governing the formation of the *Ciona* tadpole to identify homologous structures in hemichordates and echinoderms. For example, *FGF9/16/20*, *Mesp*, *FoxF*, and *Tolloid* constitute specialized components of the early chordate heart network (supporting online text), and it will be interesting to see if this pathway is used in echinoderms or hemichordates. Similarly, it should be possible to determine whether any of the circuits governing the compartmentalization of the *Ciona* nerve cord or cerebral vesicle are used within the apparently more diffuse nervous systems of lower Deuterostomes.

- References and Notes**
1. E. H. Davidson *et al.*, *Science* **295**, 1669 (2002).
 2. A. Stathopoulos, M. Levine, *Dev. Cell* **9**, 449 (2005).
 3. M. Loose, R. T. Patient, *Dev. Biol.* **271**, 467 (2004).
 4. N. Satoh, *Nat. Rev. Genet.* **4**, 285 (2003).
 5. P. Dehal *et al.*, *Science* **298**, 2157 (2002).
 6. H. Nishida, K. Sawada, *Nature* **409**, 724 (2001).
 7. K. S. Imai, Y. Satou, N. Satoh, *Development* **129**, 2723 (2002).
 8. K. Yagi, N. Takatori, Y. Satou, N. Satoh, *Dev. Biol.* **282**, 535 (2005).
 9. Y. Satou *et al.*, *Dev. Genes Evol.* **212**, 87 (2002).
 10. K. Imai, N. Takada, N. Satoh, Y. Satou, *Development* **127**, 3009 (2000).
 11. Y. Satou, K. S. Imai, N. Satoh, *Development* **128**, 3559 (2001).
 12. J. C. Corbo, M. Levine, R. W. Zeller, *Development* **124**, 589 (1997).
 13. K. S. Imai, N. Satoh, Y. Satou, *Development* **129**, 1729 (2002).
 14. K. S. Imai, N. Satoh, Y. Satou, *Development* **129**, 3441 (2002).
 15. V. Bertrand, C. Hudson, D. Caillol, C. Popovici, P. Lemaire, *Cell* **115**, 615 (2003).
 16. C. Hudson, H. Yasuo, *Development* **132**, 1199 (2005).
 17. K. S. Imai, K. Hino, K. Yagi, N. Satoh, Y. Satou, *Development* **131**, 4047 (2004).
 18. Because *Ci-Delta-like* (*Ci-Delta2*) (16) was missed in our previous screen and a new cDNA was obtained for *Pax3/7*, detailed expression profiles are now available for both genes (fig. S9), which revealed that *Ci-Delta-like* is expressed at and before the early gastrula stage.
 19. Materials and methods are available as supporting material on *Science* Online.
 20. L. Yamada *et al.*, *Development* **130**, 6485 (2003).
 21. We examined effects of the MO-mediated knockdown of 25 genes, with the exception of *FoxC* and *Mesp*, on the expression of 73 genes at the various cleavage stages. *FoxC*, *Mesp*, and *Jun* were not included in the expression analysis, because *FoxC*, *Mesp*, and *Jun* begin to be expressed late in the early gastrula stage; thus, their functions and expression patterns are better evaluated at later stages.
 22. The *Ciona* Integrated Database, GHOST (<http://ghost.zool.kyoto-u.ac.jp/network/TFSTgenes.html>).
 23. H. Takahashi *et al.*, *Genes Dev.* **13**, 1519 (1999).
 24. E. Agius, M. Oelgeschläger, O. Wessely, C. Kemp, E. M. De Robertis, *Development* **127**, 1173 (2000).
 25. V. Duboc, E. Rottinger, L. Besnardau, T. Lepage, *Dev. Cell* **6**, 397 (2004).
 26. M. Whitman, *Dev. Cell* **1**, 605 (2001).
 27. J. C. Corbo, A. Erives, A. Di Gregorio, A. Chang, M. Levine, *Development* **124**, 2335 (1997).
 28. N. Takatori, Y. Satou, N. Satoh, *Mech. Dev.* **116**, 235 (2002).
 29. M. Tokuoka, N. Satoh, Y. Satou, *Dev. Biol.* **288**, 387 (2005).
 30. K. Katsube, K. Sakamoto, *Int. J. Dev. Biol.* **49**, 369 (2005).
 31. S. Fujiwara, J. C. Corbo, M. Levine, *Development* **125**, 2511 (1998).
 32. This research was mainly supported by Grants-in-Aid from MEXT, Japan, and from Japan Society for the Promotion of Science (JSPS) to Y.S. (17687022 and 13044001). K.S.I. was supported by a postdoctoral fellowship from the JSPS for Japanese junior scientists with a research grant (15004751). M.L. is supported by a grant from the NIH. This research was also supported in part as a Core Research for Evolutionary Science and Technology (CREST) project by the Japan Science and Technology Agency to N.S.

Supporting Online Material

- www.sciencemag.org/cgi/content/full/312/5777/1183/DC1
- Materials and Methods
- SOM Text
- Figs. S1 to S9
- Tables S1 to S7
- References and Notes
- Database S1

5 December 2005; accepted 27 March 2006
10.1126/science.1123404

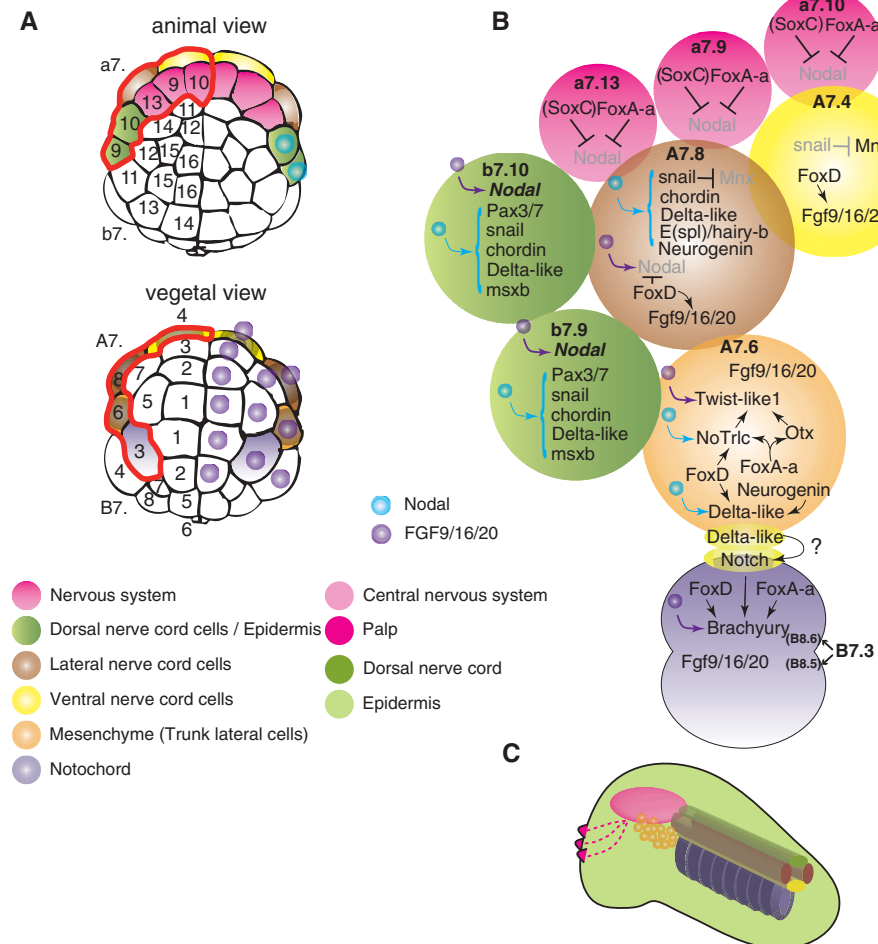


Fig. 4. The Nodal network. (A) The 64-cell embryos depicting cells secreting Nodal and FGF9/16/20 and developmental fates of selected blastomeres shown in (B). Note that cells whose ancestors express the FGF are also depicted. (B) Nodal-centered gene networks. Arrows and flattened arrows show activation and repression of downstream genes. Genes shown in gray or in parentheses are not expressed there. (C) A schematic representation of tissues of the tailbud embryo differentiated from the blastomeres shown in (B). The color codes in (A) are applied in the same way to (B) and (C). Note that only the networks related to Nodal are depicted, and some regulatory interactions seen in their ancestral cells and descendants are also included for better understanding. See the text for the details.